

Robust Linear and Nonlinear Time-Optimal Control Design Using Multiple Inputs

BY

**Dr. Bassam A. Albassam
King Saud University
College of Engineering
Mechanical Engineering Department
P.O. Box 800
Riyadh 11421
Saudi Arabia**

Email: albassam@ksu.edu.sa

Phone : (009661)467-6684

Fax : (009661) 467-6652

Robust Linear and Nonlinear Time-Optimal Control Design Using Multiple Inputs

Bassam A. Albassam

King Saud University – Mechanical Engineering Dept.

Keywords : optimal control, vibration control, robust control, nonlinear control

Abstract

The problem of designing minimum time, rest-to-rest maneuver for flexible structures is addressed. Multiple control inputs are utilized and the bang-bang control switches are calculated using the shooting method. Optimality is verified by calculating, simultaneously, the costate variables associated with the optimal control problem and then comparing the roots of the switching functions for each control input with the calculated switching times. The proposed technique is applied to the mass-spring-damper system and the effect of mass, damping and stiffness on the optimal control structure is illustrated. In addition, the developed numerical algorithm is used to calculate the time-optimal control inputs with structural uncertainty and nonlinearity.

1. Introduction

Recently, there has been a strong interest in the field of time-optimal maneuver of flexible structures. This is due to the use of lightweight materials for the purposes of both speed and fuel efficiency. The minimum time property obtained in this research is required by many applications such as robotic arms, large space structures and disk-drive heads.

In the past, research in this area has focused on developing numerical techniques for calculating the time-optimal control input using a single actuator. Scrivener and Thompson¹ have written an excellent survey paper in the field of time-optimal attitude maneuvers. Singh and Vadali² have transformed the scalar time-optimal control problem into parameter optimization by forcing the zeros of the control input to cancel the poles of the system. In the same work, the authors have also extended the technique to generate robust control input. Liu and Wie³ have developed a similar technique to calculate a robust control input by solving a parameter optimization problem subject to robustness constraints. They have also considered two one-sided control inputs in the same work, but have not proved optimality of their calculated solution. Singh et al⁴ have developed a homotopy method to calculate the switching times for the time-optimal

control input for a rigid hub with many flexible appendages. Although multiple control inputs have been considered in this study, the developed homotopy scheme is for the scalar control input case. Ben-Asher et al⁵ have transformed the time-optimal maneuvering problem with scalar control input to a problem in nonlinear programming. They have also developed a method to verify the optimality of the calculated solution. Meier and Bryson⁶ have developed a numerical method, called the switch time optimization (STO), for finding the switching times for time-optimal control inputs. Their developed algorithm is applicable to both scalar as well as multiple control inputs. The characteristics of time-optimal control input for single input flexible structures, with and without damping, have been studied by Pao⁷.

Thus far, little research has been carried out in the field of time-optimal control design for multi-input systems. Lim et al.⁸ have presented a systematic methodology for the design of multiple input shaping filters based on convex optimization techniques. Pao⁹ has extended the pole-cancellation approach developed by Singh and Vadali² to multi-input systems. Muenchhof and Singh¹⁰ have extended the pole cancellation approach to design a jerk-limited time-optimal control for multi-input systems.

This paper is concerned with the design of time-optimal control input for multi-input systems. The numerical algorithm developed for the calculations of the control inputs switching and final times are based on the shooting method. The control inputs are assumed to be saturated at all times during the maneuver resulting in a bang-bang type of control inputs. The developed numerical algorithm solves for the control inputs switching and final times as well as the initial values of the costate variables. Optimality of the calculated solution is verified by comparing the control inputs switching times with the roots of the corresponding switching functions.

This paper is organized as follows. In Section 2, the time-optimal control problem is formulated. In Section 3, a simple example with one rigid body mode and one flexible mode is chosen to demonstrate the applicability of the developed numerical algorithm. The solution method is laid out in Section 4 and the calculations of the costate variables are given in Section 5. In Section 6, an optimal solution is calculated and the effect of mass, stiffness and damping on the resulting optimal control structure is presented. The robust time-optimal control design is presented in Section 7. Then, in Section 8, the developed numerical algorithm is used to design the time-optimal control for the mass-spring system with nonlinearity. In Section 9, the time-optimal control design is obtained in the presence of both nonlinearity and structural uncertainty. The final section summarizes the results of this study.

2. Problem Formulation

A general system model can be written in state space format as

$$\dot{\vec{x}}(t) = \vec{f}(\vec{x}(t), \vec{u}(t), t) \quad (1)$$

where $\vec{x}(t)$ is an $n \times 1$ state vector, $\vec{u}(t)$ is an $m \times 1$ control input vector and t is time. Over dot symbolizes differentiating with respect to time. The system described in Eq. (1) can be linear or nonlinear, rigid or flexible. It is assumed that it is desired to transfer this system from the initial conditions $\vec{x}(0)$ to the final conditions $\vec{x}(t_f)$ in minimum time. Therefore, the optimal control problem would be to calculate the control input vector $\vec{u}(t)$ that minimizes the maneuver time

$$J = \int_0^{t_f} dt = t_f \quad (2)$$

subject to the state equations, Eqs. (1), initial and final conditions, $\vec{x}(0)$ and $\vec{x}(t_f)$ and the following control input constraints

$$\vec{u}_{\min} \leq \vec{u}(t) \leq \vec{u}_{\max} \quad (3)$$

where \vec{u}_{\min} and \vec{u}_{\max} are two vectors defining the minimum and maximum values for each control input contained in the vector $\vec{u}(t)$.

The optimal control problem solution can be obtained by first defining the Hamiltonian¹¹ H as

$$H(\vec{x}(t), \vec{\lambda}(t), \vec{u}(t), t) = 1 + \vec{\lambda}^T \vec{f}_1(\vec{x}(t), t) + \vec{\lambda}^T \vec{f}_2(\vec{x}(t), t) \vec{u}(t) \quad (4)$$

where $\vec{\lambda}(t)$ is the costate vector and

$$\vec{f}(\vec{x}(t), \vec{u}(t), t) = \vec{f}_1(\vec{x}(t), t) + \vec{f}_2(\vec{x}(t), t) \vec{u}(t) \quad (5)$$

The costate vector of differential equations can be derived using¹¹

$$\dot{\vec{\lambda}}(t) = -\frac{\partial H}{\partial \vec{x}(t)} \quad (6)$$

which results in an $n \times 1$ vector of costate variables. The initial values of the costate variables, $\vec{\lambda}(0)$, are considered to be unknowns of the optimal control problem.

Furthermore, the components of $\vec{\lambda}^T \vec{f}_2$, in Eq. (4), define m switching functions for each control input in the control input vector $\vec{u}(t)$ as

$$\phi_i = \lambda_i (f_2)_i \quad (7)$$

where ϕ_i is the switching function associated with the control input u_i , and λ_i and $(f_2)_i$ are the i^{th} component of the vectors $\vec{\lambda}$ and \vec{f}_2 , respectively.

The necessary conditions of optimality¹¹ state that the optimal solution should satisfy the state equations, Eqs. (1), with its associated initial and final conditions, the costate equations, Eqs. (6), the control constraints in Eqs. (3) and the transversality condition which is defined later in Eq. (8).

In order to develop a numerical algorithm to solve for the optimal solution, it is assumed that all the control inputs are saturated during the maneuver. This assumption is a realistic one since bang-bang control inputs utilize the maximum power available from the actuators to achieve fast maneuver. It is noted that a switching function ϕ_i should have roots at only the switching times of the control input u_i . Consequently, the resulting unknowns of the optimal control problem would be the values of the switching times for each control input as well as the initial values of the costate variables.

One final equation that the optimal solution should satisfy is the transversality condition¹¹, which is defined by

$$H(t = 0) = 0 \quad (8)$$

The numerical algorithm developed¹² uses the simple shooting method to calculate the switching and final times as well as the initial values of the costate variables according to the following steps:

- (1) Assume values for the unknowns. These are the switching and maneuver times and the initial values for the costate variables.
- (2) Integrate the state equations and costate equations, Eqs. (1) and (6) and compute the errors in the final conditions, switching functions and transversality condition.
- (3) Update the unknowns so that the error in Step (2) is reduced.
- (4) Repeat Steps (2) ~ (3) until the errors in Step (2) reach a desired minimum value.

The above steps are now demonstrated in details in the following example.

3. Numerical Example

The proposed technique is demonstrated on a simple system with one rigid body mode and one flexible mode as shown in Fig. 1. Even though a flexible system with only one rigid body mode and one flexible mode is considered, it is emphasized that the proposed numerical technique is neither limited in the number of inputs nor in the number of modes. The equations of motion for this system, in matrix form, is

$$\begin{bmatrix} m_1 & 0 \\ 0 & m_2 \end{bmatrix} \begin{Bmatrix} \ddot{x}_1 \\ \ddot{x}_2 \end{Bmatrix} + \begin{bmatrix} c & -c \\ -c & c \end{bmatrix} \begin{Bmatrix} \dot{x}_1 \\ \dot{x}_2 \end{Bmatrix} + \begin{bmatrix} k & -k \\ -k & k \end{bmatrix} \begin{Bmatrix} x_1 \\ x_2 \end{Bmatrix} = \begin{bmatrix} 1 & 0 \\ 0 & 1 \end{bmatrix} \begin{Bmatrix} u_1 \\ u_2 \end{Bmatrix} \quad (9)$$

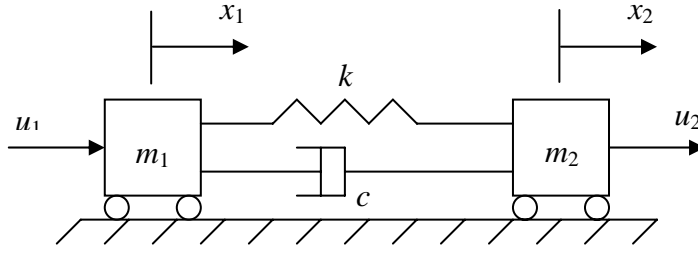


Fig. 1 Simplified system model.

Using the modal matrix P normalized with respect to the mass matrix,

$$P = \begin{bmatrix} \frac{1}{\sqrt{m_1 + m_2}} & -\sqrt{\frac{m_2}{m_1(m_1 + m_2)}} \\ \frac{1}{\sqrt{m_1 + m_2}} & \sqrt{\frac{m_1}{m_2(m_1 + m_2)}} \end{bmatrix} \quad (10)$$

the above system can be transformed to

$$\begin{aligned} \ddot{\theta} &= a_1 u_1 + a_2 u_2 \\ \ddot{q} + 2\zeta\omega \dot{q} + \omega^2 q &= a_3 u_1 + a_4 u_2 \end{aligned} \quad (11)$$

where $\theta(t)$ is the rigid body coordinate and $q(t)$ is the flexible coordinate and ζ and ω are the damping ratio and natural frequency, respectively. The coefficients in Eqs. (11) are derived using the transformation matrix, Eq. (10), that gives

$$\begin{aligned} a_1 &= \frac{1}{\sqrt{m_1 + m_2}} & , & & a_2 &= \frac{1}{\sqrt{m_1 + m_2}} \\ a_3 &= -\sqrt{\frac{m_2}{m_1(m_1 + m_2)}} & , & & a_4 &= \sqrt{\frac{m_1}{m_2(m_1 + m_2)}} \\ \omega &= \sqrt{\frac{k(m_1 + m_2)}{m_1 m_2}} & , & & \zeta &= \frac{c}{2} \sqrt{\frac{m_1 + m_2}{k m_1 m_2}} \end{aligned} \quad (12)$$

Equations (11) can be written in state space format as

$$\begin{aligned} \dot{\theta}_1 &= \theta_2 \\ \dot{\theta}_2 &= a_1 u_1 + a_2 u_2 \\ \dot{q}_1 &= q_2 \\ \dot{q}_2 &= -\omega^2 q_1 - 2\zeta\omega q_2 + a_3 u_1 + a_4 u_2 \end{aligned} \quad (13)$$

where $\theta_1 = \theta$, $\theta_2 = \dot{\theta}$, $q_1 = q$ and $q_2 = \dot{q}$.

The optimal control problem is solved using the developed numerical algorithm to find the optimal control inputs $u_1(t)$ and $u_2(t)$ that minimizes the maneuver time t_f subject to the equations of motion, Eqs. (9), and the following rest-to-rest boundary conditions,

$$\begin{aligned} x_1(0) = \dot{x}_1(0) = 0 & \quad , \quad x_1(t_f) = x_f \quad , \quad \dot{x}_1(t_f) = 0 \\ x_2(0) = \dot{x}_2(0) = 0 & \quad , \quad x_2(t_f) = x_f \quad , \quad \dot{x}_2(t_f) = 0 \end{aligned} \quad (14)$$

where x_f is the desired final position, in meters, for the two masses. These boundary conditions can be transformed from physical to modal coordinates using the transformation in Eq. (10) to give

$$\begin{aligned}\theta_1(0) = \theta_2(0) = 0, \quad \theta_1(t_f) = \theta_f, \quad \theta_2(t_f) = 0 \\ q_1(0) = q_2(0) = 0, \quad q_1(t_f) = q_2(t_f) = 0\end{aligned}\tag{15}$$

where θ_f is given by

$$\theta_f = \sqrt{m_1 + m_2} x_f\tag{16}$$

Furthermore, the calculated control inputs should satisfy the following constraints

$$-u_{1\max} \leq u_1(t) \leq u_{1\max}, \quad -u_{2\max} \leq u_2(t) \leq u_{2\max}\tag{17}$$

where it is assumed that $u_{i\min} = -u_{i\max}$, $i = 1, 2$.

4. Method of Solution

The control inputs $u_1(t)$ and $u_2(t)$ are assumed to be saturated at all times during the maneuver. This assumption is a consequence of the fact that the control inputs utilize the maximum power available from the actuator to achieve fast maneuver. Consequently, the control inputs have the structures shown in Fig. (2). The number as well as the values of the switching times are generally different for each control input and are unknown a priori. The dotted lines indicate that the number of control switching times may be more than what is shown in Fig. (2). Unfortunately, no proven theory exists that specifies the number of control switching times for flexible structures. This is one of the main obstacles to face when solving time-optimal control problems for flexible structures. Therefore, in this paper, the number of switching times is assumed first based on results of previous research articles^{2,3,4,5,7} using only a single control input. Alternatively, one can assume any number for the switching times to start the algorithm, and then either of two possibilities can happen. The numerical algorithm may not converge to a solution, which is a possible indication that the assumed number of switching times is not optimal. The second possibility is that the numerical algorithm converges to a solution that is not optimal. This means that the computed switching times do not match with the roots of the computed switching function. This is again another indication that the assumed number of switching times is not optimal. Instead, one can use some of the direct methods^{13,14} that solve optimal control problems and are easy to implement to have some insight into the optimal control structure. These direct methods are generally not accurate but can give some insight about the optimal control structure.

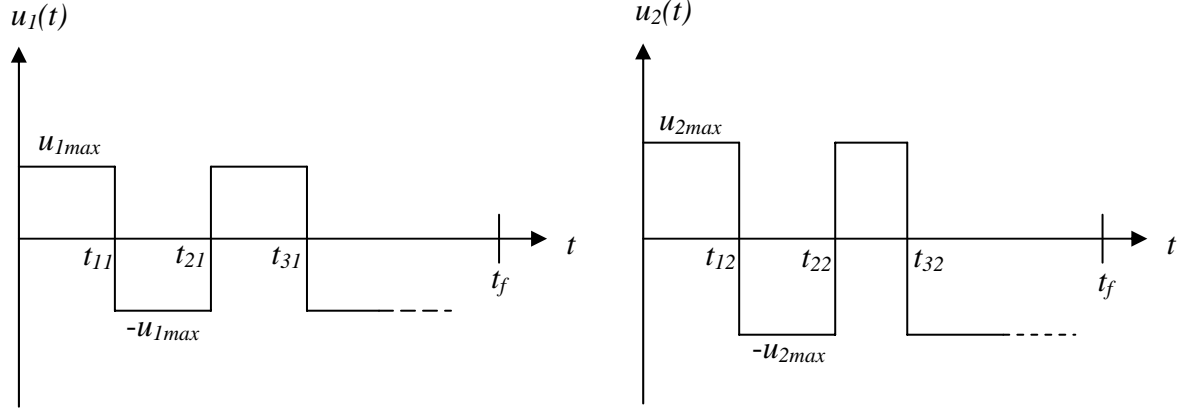


Fig. 2 Control inputs structures.

5. Calculation of Costate Variables

The time optimality of the state solution is proved with the help of calculating, simultaneously, the costate variables. The Hamiltonian¹¹ H of the system can be written as

$$\begin{aligned} H &= 1 + \lambda_1 \dot{\theta}_1 + \lambda_2 \dot{\theta}_2 + \lambda_3 \dot{q}_1 + \lambda_4 \dot{q}_2 \\ &= 1 + \lambda_1 \theta_2 + \lambda_2 (a_1 u_1 + a_2 u_2) + \lambda_3 q_2 + \lambda_4 (-\omega^2 q_1 - 2\zeta\omega q_2 + a_3 u_1 + a_4 u_2) \end{aligned} \quad (18)$$

where $\lambda_i(t)$ is the i^{th} costate variable and should satisfy

$$\begin{aligned} \dot{\lambda}_1 &= -\frac{\partial H}{\partial \theta_1} &\Rightarrow \dot{\lambda}_1 &= 0 \\ \dot{\lambda}_2 &= -\frac{\partial H}{\partial \theta_2} &\Rightarrow \dot{\lambda}_2 &= -\lambda_1 \\ \dot{\lambda}_3 &= -\frac{\partial H}{\partial q_1} &\Rightarrow \dot{\lambda}_3 &= \omega^2 \lambda_4 \\ \dot{\lambda}_4 &= -\frac{\partial H}{\partial q_2} &\Rightarrow \dot{\lambda}_4 &= -\lambda_3 + 2\zeta\omega \lambda_4 \end{aligned} \quad (19)$$

The switching functions ϕ_1 and ϕ_2 for each control input u_1 and u_2 , respectively, are given by

$$\begin{aligned} \phi_1 &= a_1 \lambda_2 + a_3 \lambda_4 \\ \phi_2 &= a_2 \lambda_2 + a_4 \lambda_4 \end{aligned} \quad (20)$$

Furthermore, the transversality condition¹¹ is given by

$$H(0) = 0 \Rightarrow 1 + \lambda_2(0)(a_1 u_{1\max} + a_2 u_{2\max}) + \lambda_4(0)(a_3 u_{1\max} + a_4 u_{2\max}) = 0 \quad (21)$$

where it is assumed that each control input starts with positive value.

The initial values for the costate variables are unknowns of the problem and can be calculated either after or simultaneously with the calculation of the switching times. Specifically, the following steps are used to determine the missing initial costates:

- (1) Select starting values for the initial values of the costate variables
- (2) Integrate the costate differential equations, Eqs. (19)
- (3) Evaluate the transversality condition, Eq. (21), at the initial time and the switching functions, Eqs. (20), at each switching time. The switching function ϕ_i should be equal to zero at each switching time t_{ji} corresponding to the control input u_i , $i=1$ or 2 and $j=1,2,3\dots$
- (4) Update the initial costate variables to satisfy the transversality condition as well as the switching functions.
- (5) Terminate the algorithm when the transversality condition as well as the switching functions are practically satisfied.

Finally, the optimality of the state space solution is verified by comparing the control inputs switching times with the roots of the switching functions.

6. Numerical Results

6.1 Undamped System

The values for the parameters of the system, in Eqs. (9), have been chosen as

$$m_1 = 1 \text{ kg} \quad m_2 = 2 \text{ kg} \quad k = 1 \text{ N/m} \quad c = 0 \text{ N/(m/s)} \quad (22)$$

so that

$$\omega_{\text{rigid}} = 0 \quad \omega = \sqrt{1.5} \quad (23)$$

where ω_{rigid} and ω are the natural frequencies, in rad/s, of the system for the rigid body mode and flexible mode, respectively. In addition, the maximum control magnitudes for each control input, $u_{1\text{max}}$ and $u_{2\text{max}}$, are set to 1 N. The optimal solution for a maneuver distance, x_f , of one meter is shown in Fig. (3). Figure (3) shows a complete agreement between the control inputs switching times and the roots of their corresponding switching functions, thereby, proving optimality of the solution. The computed switching times, in seconds, for each control input are shown in Table 1.

Table 1. Switching times for control inputs u_1 and u_2 .

Control Input	First Switch	Second Switch	Third Switch	Maneuver Time
u_1	0.7505	1.3746	1.9986	2.7491
u_2	1.3746			

Control input u_1 has three switches whereas control input u_2 has only one switch. The symmetry property⁴ about mid-maneuver time noted for a single control input has also been preserved when using two control inputs. As a result, the second switching time for the first control input u_1 is identical to the first switching time for the second control

input u_2 . This property can be used to reduce the number of unknowns in the optimal control problem. The variations of the switching and final times as the mass m_2 changes from 2 kg to 1 kg are shown in Fig. (4). Figure (4) shows that the maneuver becomes faster as the mass m_2 decreases, as a result of the decrease in the inertia forces. Furthermore, this figure shows an interesting characteristic in which the values for the first, second and third switching times for the first control input approach each other and coincide with each other to become only one switching time when the values of the two masses are equal. To investigate this point further, the system equations of motion in modal coordinates, for $m_1 = m_2 = 1$ kg, are given by

$$\begin{aligned}\ddot{\theta} &= -\frac{1}{\sqrt{2}}u_1 - \frac{1}{\sqrt{2}}u_2 \\ \ddot{q} + 2q &= -\frac{1}{\sqrt{2}}u_1 + \frac{1}{\sqrt{2}}u_2\end{aligned}\tag{24}$$

Therefore, if both control inputs have the same saturation limit (i.e., $u_{1max} = u_{2max}$) and their switching and final times are equal, then both control inputs are identical and Eqs. (24) reduce to

$$\begin{aligned}\ddot{\theta} &= -\frac{2}{\sqrt{2}}u \\ \ddot{q} + 2q &= 0\end{aligned}\tag{25}$$

where $u(t) = u_1(t) = u_2(t)$. Equations (25) reveal that the flexible mode, in this case, is not being excited and, therefore, the system moves like a rigid body with an equivalent mass equals to $\sqrt{2}/2$ kg. In this case an analytical solution¹⁵ for the switching and final times exists which is given by

$$t_1 = \sqrt{\frac{\theta(t_f)}{b \times u_{max}}} \quad t_f = 2 \times t_1\tag{26}$$

where b is the coefficient of u in the first equation of Eqs. (25), $\theta(t_f)$ is the rigid-body coordinate at the final time t_f , given in Eq. (16), and u_{max} is the maximum saturation limit for both control inputs. Equations (26) result in a switching time $t_1 = 1$ s and a maneuver time $t_f = 2$ s, which agrees with the calculated switching and maneuver times, using the developed numerical algorithm, as seen in Fig. (4). In this case, all the energy transferred to the system from the control inputs is utilized to perform the maneuver while no energy is lost in the vibrations caused by exciting the flexible mode. Generally, if the absolute values of a_3 and a_4 , in Eqs. (12), are equal and both control inputs have the same maximum saturation limit, u_{max} , then the minimum time maneuver is performed for an equivalent rigid body system described by only the first equation of Eqs. (11). In this case, Eqs. (26) can be used to calculate the switching and maneuver

times. Therefore, if the following condition

$$\frac{m_1}{u_{1\max}} = \frac{m_2}{u_{2\max}} \quad (27)$$

is satisfied then the control inputs are able to perform the rigid body maneuver with one equal switching time for both control inputs. Furthermore, the time-optimal solution, in this case, does not depend on the values of damping c nor stiffness k . Therefore, when the condition in Eq. (27) is satisfied the resulting time-optimal solution is very robust with respect to changes in the parameters k and c .

The effect of varying the stiffness k from 0.01 to 300 N/m on the time-optimal switching and maneuver times while keeping the values of the rest of the parameters as in Eqs. (22) is shown in Fig. (5). Clearly this figure indicates that the maneuver time decreases as k is increased. Figure (5) also shows that the rate of maneuver time decrease is higher for low values of k . This is due to the system gradually approaching a rigid body, where all the energy transferred to the system from the actuators is utilized into performing the minimum time maneuver. In addition, both control inputs $u_1(t)$ and $u_2(t)$ have only one switch time that are equal and located at the middle of the maneuver. In this case, solving the system equations of motion in modal coordinates, analytically, gives the following states at the final time t_f

$$\begin{aligned} \theta_1(t_f) &= \frac{1}{4} u_{\max} t_f^2 (a_1 + a_2) \\ \theta_2(t_f) &= 0 \\ q_1(t_f) &= \frac{1}{\omega^2} u_{\max} (a_5 + a_6) \left[2 \cos\left(\frac{\omega t_f}{2}\right) - \cos(\omega t_f) - 1 \right] \\ q_2(t_f) &= \frac{1}{\omega} u_{\max} (a_5 + a_6) \left[-2 \sin\left(\frac{\omega t_f}{2}\right) + \sin(\omega t_f) \right] \end{aligned} \quad (28)$$

As the value of the stiffness k goes to infinity, the frequency ω , as seen from Eqs. (12), goes to infinity too, and therefore, the third and fourth equations of Eqs. (28), representing the flexible modes in modal coordinates, go to zero. This means that the flexible modes are not excited and the system behaves like a rigid body. In this case, the values of the control switching and maneuver times can be calculated using

$$t_1 = \sqrt{\frac{\theta_1(t_f)}{u_{\max} (a_1 + a_2)}} \quad t_f = 2 \times t_1 \quad (29)$$

Substituting the values -1.7321 , -0.5774 and -0.5774 for $\theta_1(t_f)$, a_1 and a_2 , respectively, which corresponds to the parameters values in Eqs. (22), results in $t_1 = 1.2247$ s and $t_f = 2.4495$ s, which agrees with the calculated switching and maneuver times as seen in Fig.

(5).

Furthermore, Fig. (5) shows that for some values of stiffness k the three control switches for u_1 combine into only one switch. This phenomenon can be analyzed by examining Eqs. (28). The two control inputs u_1 and u_2 having only one and equal switch time as well as maneuver time mean that the system undergoes rigid-body maneuver. Consequently, the third and fourth equations in Eqs. (28) should equal to zeros. It is not difficult to prove that when the maneuver time t_f satisfies the following relation

$$t_f = n \frac{2\pi}{\omega} \quad n = 2, 4, 6, 8, \dots \quad (30)$$

then the flexible coordinates, represented by $q_1(t)$ and $q_2(t)$ in Eqs. (28), are equal to zeros. Therefore, all the values of stiffness k that satisfy the condition in Eq. (30) results in a time-optimal control inputs $u_1(t)$ and $u_2(t)$ with only one equal switch time. Hence, all the crossing points in Fig. (5) correspond to values of stiffness k satisfying the relation in Eq. (30). Substituting for the maneuver time t_f from Eqs. (29), the natural frequency ω and a_1 and a_2 from Eqs. (12), and Eq. (16) for $\theta_1(t_f)$, one can obtain a simple relation for the values of stiffness k at the crossing points in Fig. (5) as

$$k = \frac{2n^2\pi^2 m_1 m_2 u_{max}}{(m_1 + m_2)^2 x_f}, \quad n = 2, 4, 6, 8, \dots \quad (31)$$

Substituting for $m_1=1$ kg, $m_2=2$ kg, $u_{max}= 1$ N, $x_f = 1$ m and $n = 2, 4,$ and 6 gives $k = 17.546, 70.184$ and 157.914 N/m, which agrees with the first three crossings in Fig. (5).

Another important factor to check when increasing the stiffness k is the energy that has transferred to both the rigid body mode and the flexible mode. As the energy transferred to the rigid body mode is increased at the expense of transferring less energy to the flexible mode, then a faster maneuver can be achieved. The energy transferred, in Joules, to the rigid body mode, denoted by E_r , and to the flexible mode, denoted by E_f , can be calculated using

$$\begin{aligned} E_r &= \frac{1}{2} \dot{\theta}(t)^2 \\ E_f &= \frac{1}{2} (\dot{q}(t)^2 + \omega^2 q(t)^2) \end{aligned} \quad (32)$$

Averages of these energies can be calculated using

$$\begin{aligned} (E_r)_{av} &= \frac{1}{t_f} \int_0^{t_f} E_r(t) dt \\ (E_f)_{av} &= \frac{1}{t_f} \int_0^{t_f} E_f(t) dt \end{aligned} \quad (33)$$

while the percentage of energies transferred to the rigid body mode as well as to the

flexible mode are calculated using

$$\begin{aligned} \% E_r &= \frac{(E_r)_{av}}{(E_r)_{av} + (E_f)_{av}} \\ \% E_f &= \frac{(E_f)_{av}}{(E_r)_{av} + (E_f)_{av}} \end{aligned} \quad (34)$$

The percentage of energies to the total energy transferred to the rigid body and flexible modes are shown in Fig. (6). Figure (6) shows that the increase in the stiffness of the spring k increases the energy transferred to the rigid body mode at the expense of transferring less energy to the flexible mode, thereby, resulting in a faster maneuver.

6.2 Damped System

Since every structure contains damping, we consider the effect of adding damping on the time-optimal solution. Once again, the maneuver is to be achieved using two control inputs u_1 and u_2 . Assuming one switching time for one control input and three switching times for the other control input, the nine unknowns of the time-optimal control problem are the four switching times, maneuver time, and four initial values of the costate variables. The switching time t_{ji} denotes the j^{th} switching time associated with the i^{th} control input. As stated earlier, the number of unknowns of the optimal control problem should match the number of available equations. The nine equations for this problem are

$$\begin{aligned} \theta(t_f) = \theta_f, \quad \dot{\theta}(t_f) = 0, \quad q(t_f) = 0, \quad \dot{q}(t_f) = 0 \\ \phi_1(t_{11}) = 0, \quad \phi_2(t_{12}) = 0, \quad \phi_2(t_{22}) = 0, \quad \phi_2(t_{32}) = 0, \quad TC \end{aligned} \quad (35)$$

where $\phi_i(t_{ji})$ denotes the switching function at the switching time t_{ji} associated with the i^{th} control input and TC denotes the transversality condition given in Eq. (21). It is assumed here that control input u_1 has only one switch whereas control input u_2 has three switches. Equations (13) can be integrated symbolically, using for example the symbolic toolbox in Matlab¹⁶, to obtain analytical functions for the variables in Eqs. (35) in terms of the initial conditions as well as the control inputs switching and final times.

As an example, we choose the following values for the parameters

$$m_1 = 2 \text{ kg}, \quad m_2 = 1 \text{ kg}, \quad k = 1 \text{ N/m}, \quad c = 0.1 \text{ N/(m/s)}, \quad u_{max} = u_{2max} = u_{max} = x_f = 1 \quad (36)$$

The time-optimal solution for the system states and the control inputs along with their associated switching functions are given in Figs. (7) and (8), respectively. The computed control inputs switching and final times, in seconds, are shown in Table 2. It is clear from these figures that the presence of damping has eliminated the symmetry of

both control inputs about the mid-maneuver time compared with the undamped case. The effect of increasing the damping c from 0 to 5 N.s/m on the switching and final times is shown in Fig. (9). It is seen that as damping is increased, the maneuver time t_f is decreased. As damping is increased, the system becomes like a rigid body and more energy is transferred to the rigid body mode while less energy is transferred to the flexible mode. Figure (10) shows the percentages of energy transfers to the rigid body mode and the flexible mode when damping is increased. The rate of decrease of the maneuver time is higher for low damping and almost vanishes for high damping. The structure for the control input u_1 experiences some changes when damping is increased. The control input u_1 started with three switching times at low values of damping until approximately a damping value of 0.8676 N.s/m is reached. During this interval, the third switching time t_{31} and the maneuver time t_f approach each other until they become equal when the damping c equals to 0.8676 N.s/m, after which, the control input u_1 contains only two switching times. Afterwards, the control input u_1 continues to have two switching times with the second switching time t_{21} becomes very close to the maneuver time t_f , and in the limit as damping approaches infinity the system behaves like a rigid body with the control input u_1 having only one switching time. Furthermore, the first switching time for the control input u_1 becomes nearly equal to the first switching time for the control input u_2 and both approach the mid maneuver time as a result of the system behaving like a rigid body when damping is increased. The structure for the second control input u_2 remains unchanged with only one switching time for all values of damping.

Table 2. Switching times for control inputs u_1 and u_2 .

Control Input	First Switch	Second Switch	Third Switch	Maneuver Time
u_1	1.3561			2.7483
u_2	0.8179	1.4933	2.0676	

7. Robust Time-Optimal Control Design

7.1 Introduction

In this section, the sensitivity concept is used to design robust time-optimal control inputs with structural uncertainty. It is desired from the multiple control inputs, u_1 and u_2 , to perform a minimum time maneuver and at the same time minimize the sensitivity of the final states of a dynamic system to errors in estimated parameters of the system. The sensitivity of the final states of a dynamic system

$$\dot{\vec{x}} = \vec{f}(\vec{x}, \vec{u}, p, t) \quad (37)$$

to the parameter p can be determined using the finite difference approach, leading to the equation

$$\vec{S}_p = \frac{d\vec{x}(p)}{dp} = \frac{\vec{x}(p + \delta p) - \vec{x}(p)}{\delta p} \quad (38)$$

where \vec{S}_p is the sensitivity vector of the states to the parameter p . The state sensitivities can also be calculated using direct differentiation of the state equation as

$$\frac{d\dot{\vec{x}}}{dp} = \frac{\partial \vec{f}}{\partial p} + \sum_{i=1}^n \frac{\partial \vec{f}}{\partial x_i} \frac{\partial x_i}{\partial p} \quad (39)$$

Equation (39) results in a system of first order differential equations in the state sensitivities that can be combined with the state equations, Eq. (1) and solved simultaneously to yield a robust, time-optimal maneuver. Obviously, this approach leads to exact estimate of the state sensitivities compared with the finite difference approach that depends on the perturbation size δp . Robust time-optimal control design can be achieved by forcing the sensitivities to be equal to zero at the final time. The combined system of state equations and state sensitivities has the same format as the original system and, therefore, can be solved using the developed approach in Section 2.

7.2 Numerical Example

The robust control design approach is demonstrated on the two-mass-spring system, shown in Fig. (1) with parameters defined in Eq. (22). Assume that there is a degree of uncertainty about the value of stiffness k . Therefore, it is desired to design the multiple control inputs, $u_1(t)$ and $u_2(t)$, to achieve minimum time maneuver while being robust against variations in the stiffness k .

In this case, the state sensitivities of the system defined in Eqs. (9) to the parameter k can be derived using Eq. (39) to give

$$\begin{aligned} \dot{x}_{1s} &= x_{3s} \\ \dot{x}_{2s} &= x_{4s} \\ \dot{x}_{3s} &= -\frac{1}{m_1}(x_1 - x_2) - \frac{k}{m_1}(x_{1s} - x_{2s}) \\ \dot{x}_{4s} &= \frac{1}{m_2}(x_1 - x_2) + \frac{k}{m_2}(x_{1s} - x_{2s}) \end{aligned} \quad (40)$$

where x_{is} , $i=1..4$, denotes the state sensitivity $\frac{dx_i}{dk}$. Equation (40) can be simplified to

$$m_1 \ddot{x}_{1s} = -m_2 \ddot{x}_{2s} \quad (41)$$

which can also results in

$$\begin{aligned}\dot{x}_{2s} &= -\frac{m_1}{m_2} \dot{x}_{1s} \\ x_{2s} &= -\frac{m_1}{m_2} x_{1s}\end{aligned}\tag{42}$$

Therefore, the following second order sensitivity equation

$$m_1 \ddot{x}_{1s} = -(x_1 - x_2) - k \left(1 + \frac{m_1}{m_2} \right) x_{1s}\tag{43}$$

with the following boundary conditions

$$\begin{aligned}x_{1s}(0) &= \dot{x}_{1s}(0) = 0 \\ x_{1s}(t_f) &= \dot{x}_{1s}(t_f) = 0\end{aligned}\tag{44}$$

are added to the state equations, Eq. (9), and boundary conditions, Eq. (14) with x_f equals to one. The robust control switching times are shown in Table 3. The robust time-optimal control inputs and corresponding switching function and the resulting state trajectories are shown in Figs. (11) and (12), respectively.

Table 3. Switching times for control inputs u_1 and u_2 .

Control Input	First Switch	Second Switch	Third Switch	Fourth Switch	Fifth Switch	Maneuver Time
u_1	0.3179	0.5744	1.4127	2.2510	2.5075	2.8255
u_2	1.4127					

The effect of varying the stiffness k on the state trajectory x_1 , representing the position of the mass m_1 , for the non-robust and robust control design cases is shown in Figs. (13) and (14), respectively. The robust control design shows insensitive performance while the non-robust case results in residual oscillations that can continue for a long time if damping is small.

8. Nonlinear Time-Optimal Control Design

In this section, a hard spring nonlinearity characteristics is added to the system in Fig. (1) but without damping to yield the following equations of motion

$$\begin{aligned}m_1 \ddot{x}_1 + k_1(x_1 - x_2) + \frac{1}{3}k_2(x_1 - x_2)^3 &= u_1 \\ m_2 \ddot{x}_2 + k_1(x_2 - x_1) + \frac{1}{3}k_2(x_2 - x_1)^3 &= u_2\end{aligned}\tag{45}$$

where k_2 is the stiffness of the hard spring.

It is desired, using the developed numerical technique, to design the multiple controllers, u_1 and u_2 , to perform a time-optimal rest-to-rest maneuver. The parameters of the system are given in Eq. (46). The boundary conditions for a one-unit

displacement transfer of the system are as given in Eq. (14). The resulting time-optimal switching times for the controllers are presented in Table 4. The time-optimal control inputs along with their corresponding switching functions and the resulting state trajectories are shown in Figs. (15) and (16), respectively.

$$m_1 = 1 \text{ Kg} \quad m_2 = 5 \text{ Kg} \quad k_1 = 1 \text{ N/m} \quad k_2 = 1 \text{ N/m} \quad (46)$$

Table 4. Switching times for control inputs u_1 and u_2 .

Control Input	First Switch	Second Switch	Third Switch	Maneuver Time
u_1	0.9523	2.0507	3.1496	4.1020
u_2	2.0507			

9. Robust Nonlinear Time-Optimal Control Design

The capability of this design method can also be demonstrated to design a robust time-optimal control inputs for nonlinear systems. Assume that there is uncertainty in the value of stiffness k_1 in the system given in Eqs. (45). The state sensitivity with respect to k_1 can be easily derived using the same mathematical procedure outlined in Section 7, which is given by the following second-order differential equation

$$m_1 \ddot{x}_{1s} = -(x_1 - x_2) - k_1 \left(1 + \frac{m_1}{m_2}\right) x_{1s} - k_2 (x_1 - x_2)^2 \left(1 + \frac{m_1}{m_2}\right) x_{1s}, \quad (47)$$

where $x_{1s} = dx_1/dk_1$ is the sensitivity of the state x_1 with respect to k_1 . The sensitivity of the states x_1 and x_2 with respect to k_1 are related through

$$x_{2s} = -\frac{m_1}{m_2} x_{1s} \quad (48)$$

The state sensitivity differential equation, Eq. (47), can be augmented with the system differential equations, Eqs. (45), to calculate the multiple control inputs u_1 and u_2 that results in a robust time-optimal maneuver. The parameters of the system are given in Eq. (46). The boundary conditions for the states and state sensitivity are given in Eqs. (14) and (44), respectively, in which x_f is equal to one meter. The robust time-optimal control inputs switching times are presented in Table 5. The robust time-optimal control inputs u_1 and u_2 , along with their corresponding switching functions, and the resulting state trajectories are shown in Figs. (17) and (18), respectively. The effect of varying both stiffnesses k_1 and k_2 on the maximum amplitude of residual oscillation of state x_1 is shown in Figs. (19) and (20) for the non-robust and robust controls design cases, respectively. It is clearly seen, from these figures, that the state sensitivities due to variations of system parameter k_1 have been reduced dramatically. Alternatively, it is

possible to design robust time-optimal controllers due to variations of k_2 or even both k_1 and k_2 , simultaneously, using the same numerical algorithm outlined in Section 2.

Table 5. Switching times for control inputs u_1 and u_2 .

Control Input	First Switch	Second Switch	Third Switch	Fourth Switch	Fifth Switch	Maneuver Time
u_1	0.4262	1.0822	2.2181	3.3537	4.0100	4.4367
u_2	2.2183					

10. Conclusions

The time-optimal control problem is formulated and a general scheme numerical solution is outlined for both linear and nonlinear systems. The numerical technique relies on the special feature that optimal control problems have, in which the number of equations matches the number of unknowns. The numerical technique is then applied to compute the time-optimal control inputs for the two mass-spring-damper system with two control inputs. The costate variables are calculated to verify the optimality of the solution. The effects of both stiffness k and damping c on the time-optimal solution have been investigated, where it has been shown that increasing the stiffness or damping results in a decrease in the maneuver time. The time-optimal control structures have also experienced some changes when the stiffness or damping varies. Robust time-optimal controls are also calculated using the proposed numerical technique with simulation results illustrating the effectiveness of the design procedure.

References

- [1] Scrivener, S., and Thompson, R., "Survey of Time-Optimal Attitude Maneuvers," **Journal of Guidance, Control, and Dynamics**, Vol. 17, No. 2, 1994, pp. 225-233.
- [2] Singh, T., and Vadali, S., "Robust Time-Optimal Control: Frequency Domain Approach," **Journal of Guidance, Control, and Dynamics**, Vol. 17, No. 2, 1994, pp. 346-353.
- [3] Liu, Q., and Wie, B., "Robust Time-Optimal Control of Uncertain Flexible Spacecraft," **Journal of Guidance, Control, and Dynamics**, Vol. 15, No. 3, 1992, pp. 597-604.
- [4] Singh, G., Kabamba, P., and McClamroch, N., "Planar, Time-Optimal, Rest-to-Rest Slewing Maneuvers of Flexible Spacecraft," **Journal of Guidance, Control, and Dynamics**, Vol. 12, No. 1, 1989, pp. 71-81.
- [5] Ben-Asher, J., Burns, J., and Cliff, E., "Time-Optimal Slewing of Flexible Spacecraft," **Journal of Guidance, Control, and Dynamics**, Vol. 15, No. 2, 1992, pp. 360-367.
- [6] Meier, E., and Bryson, A., "An Efficient Algorithm for Time-Optimal Control of a Two-Link Manipulator," **Journal of Guidance, Control, and Dynamics**, Vol. 13, No. 5, 1990, pp. 859-866.
- [7] Pao, L., "Minimum-Time Control Characteristics of Flexible Structures," **Journal of Guidance, Control, and Dynamics**, Vol. 19, No. 1, 1996, pp. 123-129.
- [8] Lim, S., Stevens, H. D., and How, J. P., "Input Shaping Design for Multi-Input Flexible Systems," **Journal of Dynamic Systems, Measurement, and Control**, Vol. 121, No. 3, 1999, pp. 443-447.
- [9] Pao, L. Y., "Input Shaping Design for Flexible Systems with Multiple Actuators," *Proceedings of the 13th World Congress of the International Federation of Automatic Control*, Elsevier Science, New York, 1996, pp. 267-272.
- [10] Muenchhof, M., and Singh, T., "Desensitized Jerk Limited-Time Optimal Control of Multi-Input Systems," **Journal of Guidance, Control, and Dynamics**, Vol. 25, No. 3, 2002, pp. 474-481.
- [11] Kirk, D., Optimal Control Theory, Prentice Hall, New Jersey, 1970.
- [12] Albassam, B. A., "Optimal Near-Minimum-Time Control Design for Flexible Structures," **Journal of Guidance, Control, and Dynamics**, Vol. 25, No. 4, 2002, pp. 618-625.
- [13] Hargraves, C., and Paris, S., "Direct Trajectory Optimization Using Nonlinear Programming and Collocation," **Journal of Guidance, Control, and Dynamics**, Vol.

10, No. 4, 1987, pp. 338-342.

[14] Enright, P., and Conway, B., “Discrete Approximations to Optimal Trajectories Using Direct Transcription and Nonlinear Programming,” **Journal of Guidance, Control, and Dynamics**, Vol. 15, No. 4, 1992, pp. 994-1002.

[15] Ryan, E. P., Optimal Relay and Saturating Control System Synthesis, Peter Peregrinus, London, 1982.

[16] “Matlab User’s Guide,” MathWorks, Inc., Natick, MA, 1999.

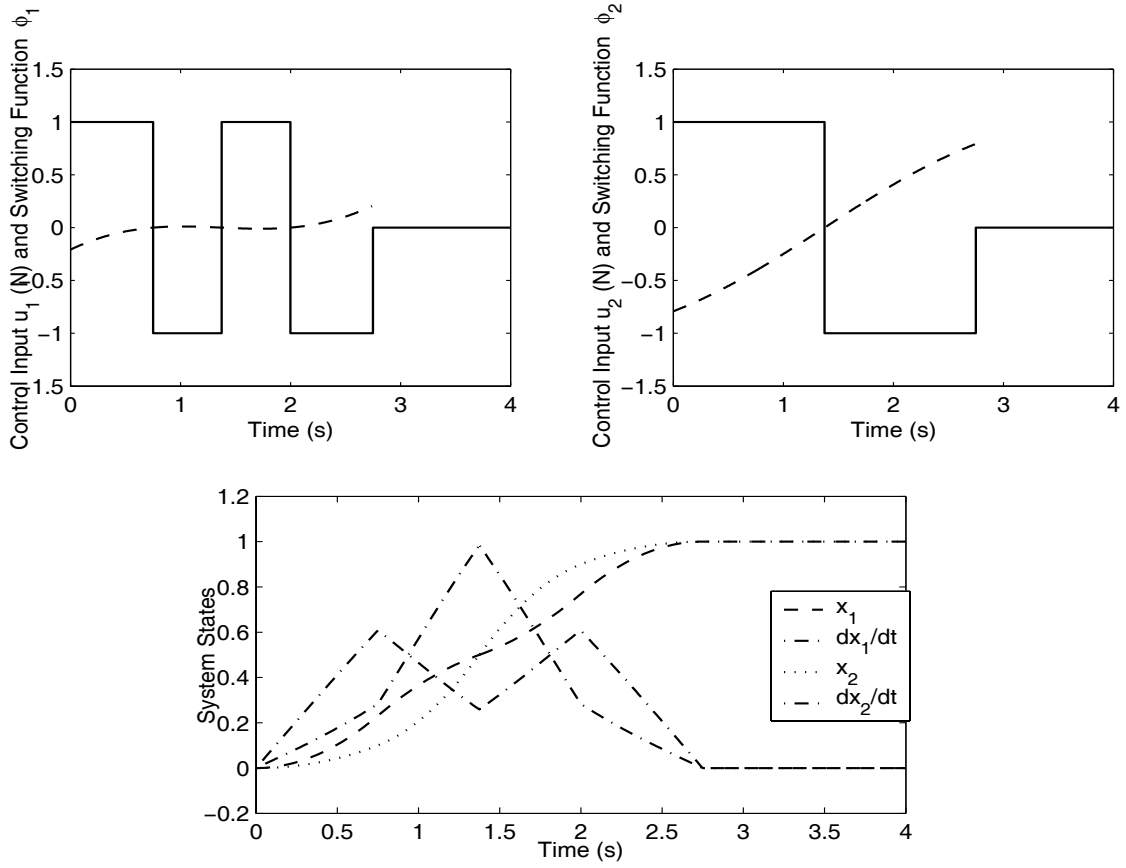


Fig. 3 Control inputs with switching functions and system states.

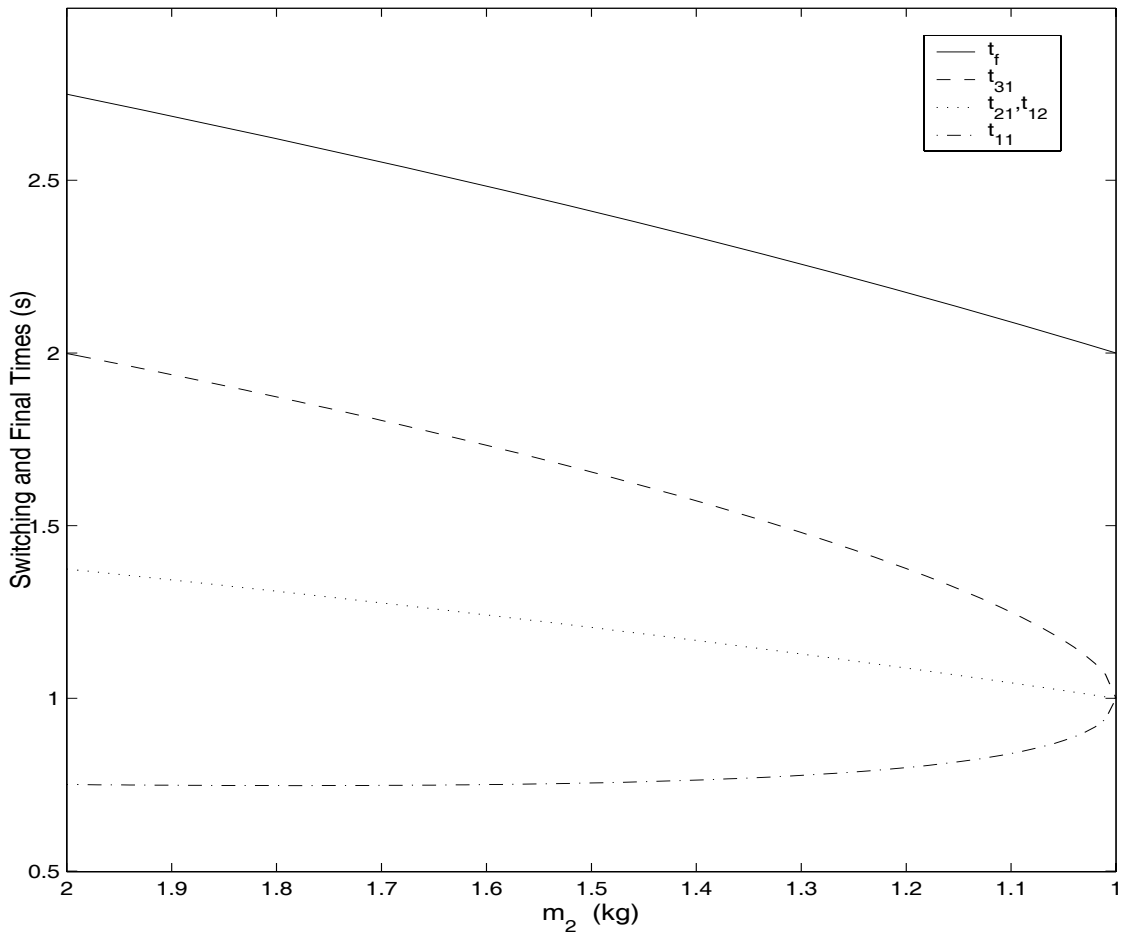


Fig. 4 Switching and final times variations as mass m_2 changes from 2 kg to 1 kg.

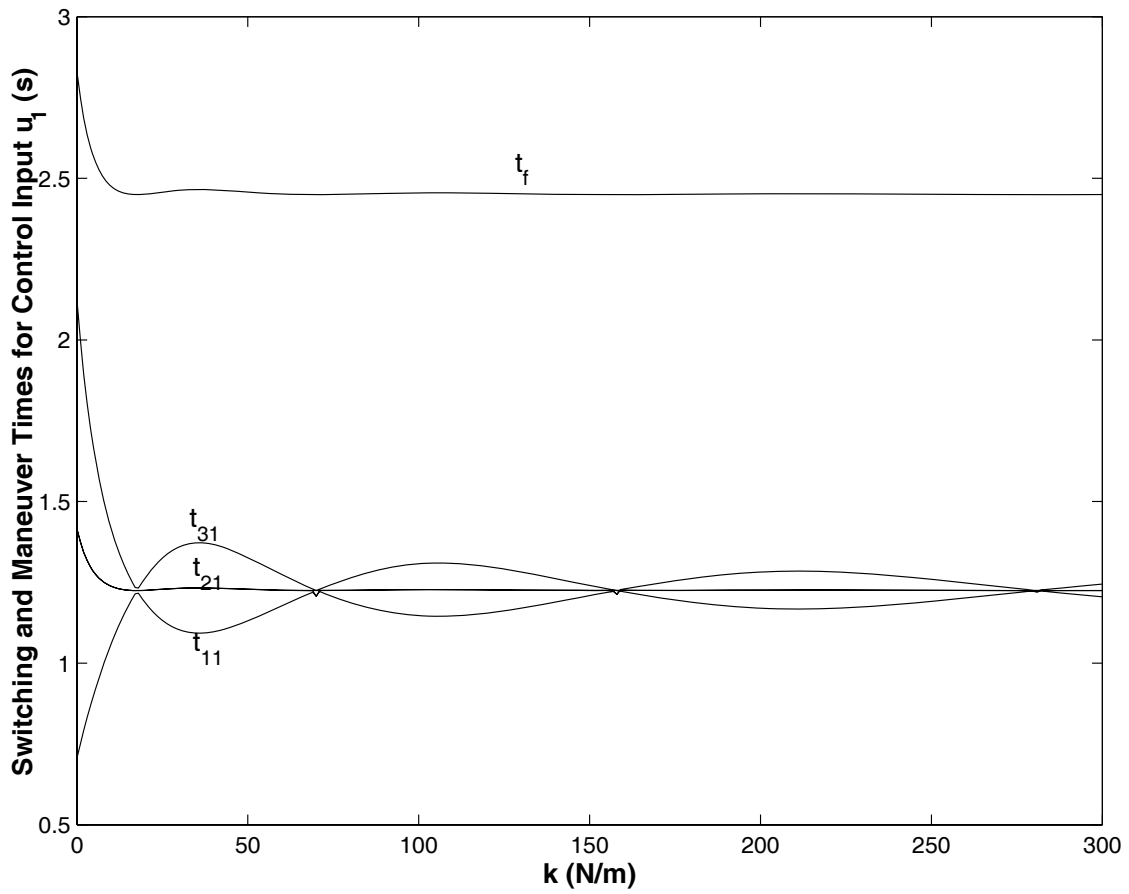


Fig. 5 Time-optimal switching and final times variations with stiffness.

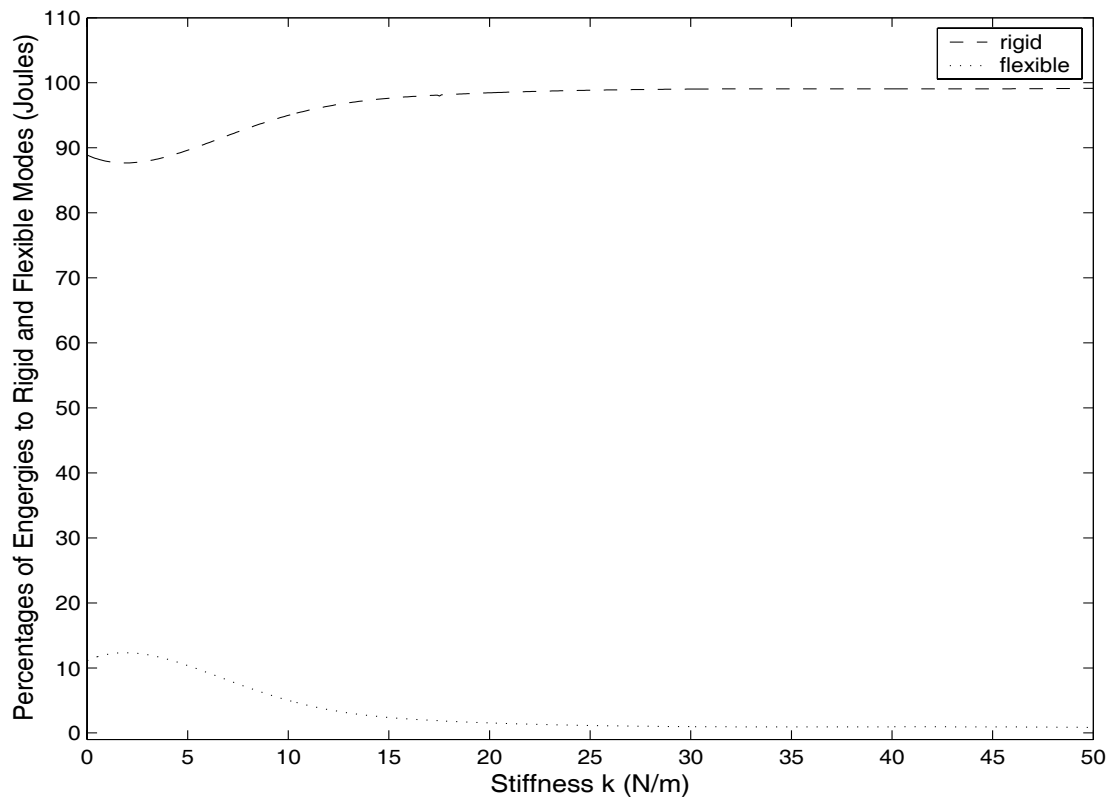


Fig. 6 Percentages of energies transferred to the rigid body and flexible modes.

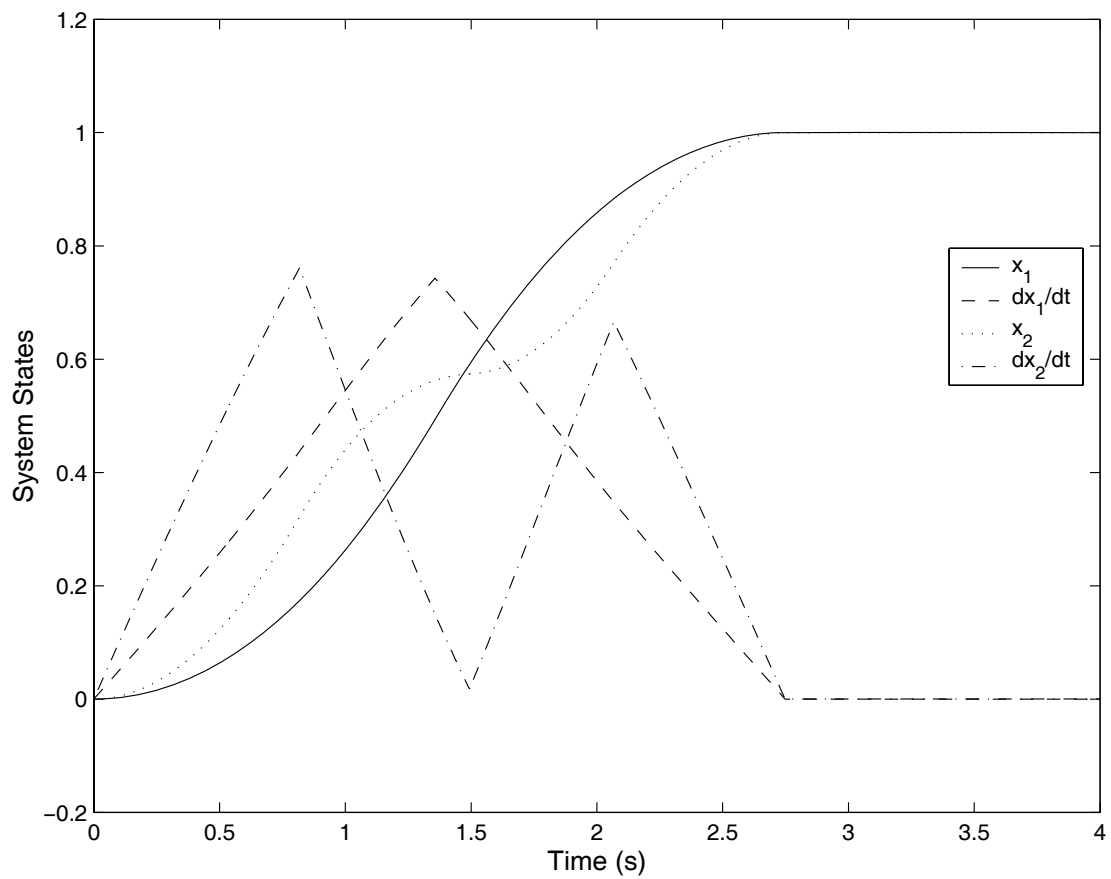


Fig. 7 Time optimal system states.

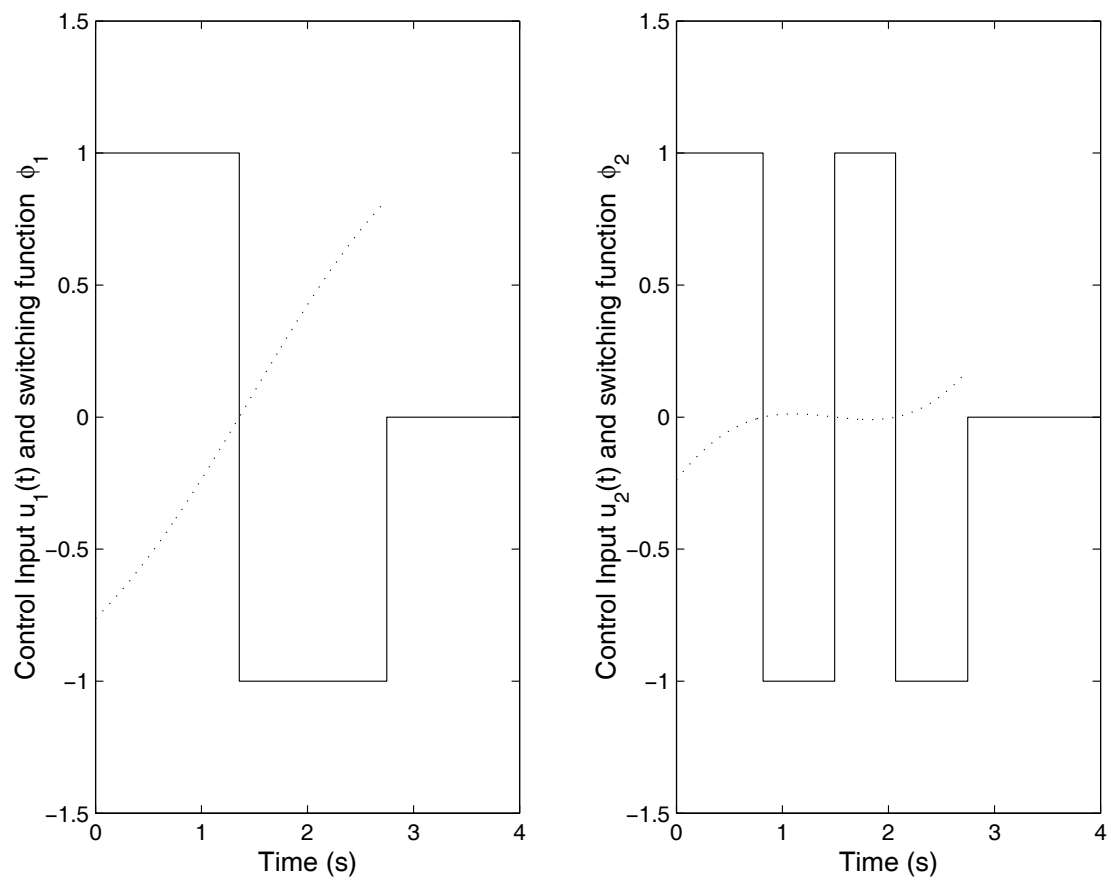


Fig. 8 Time optimal control inputs and switching functions.

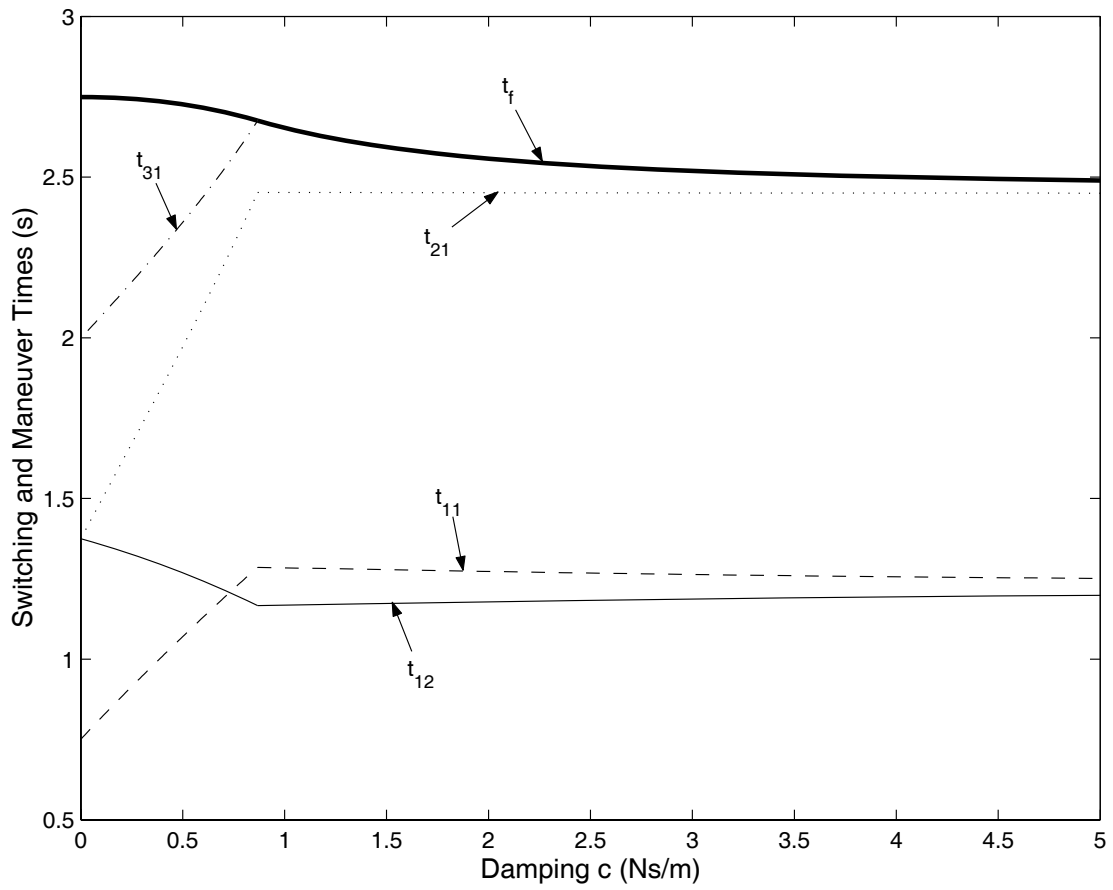


Fig. (9) Switching and maneuver times variations with damping.

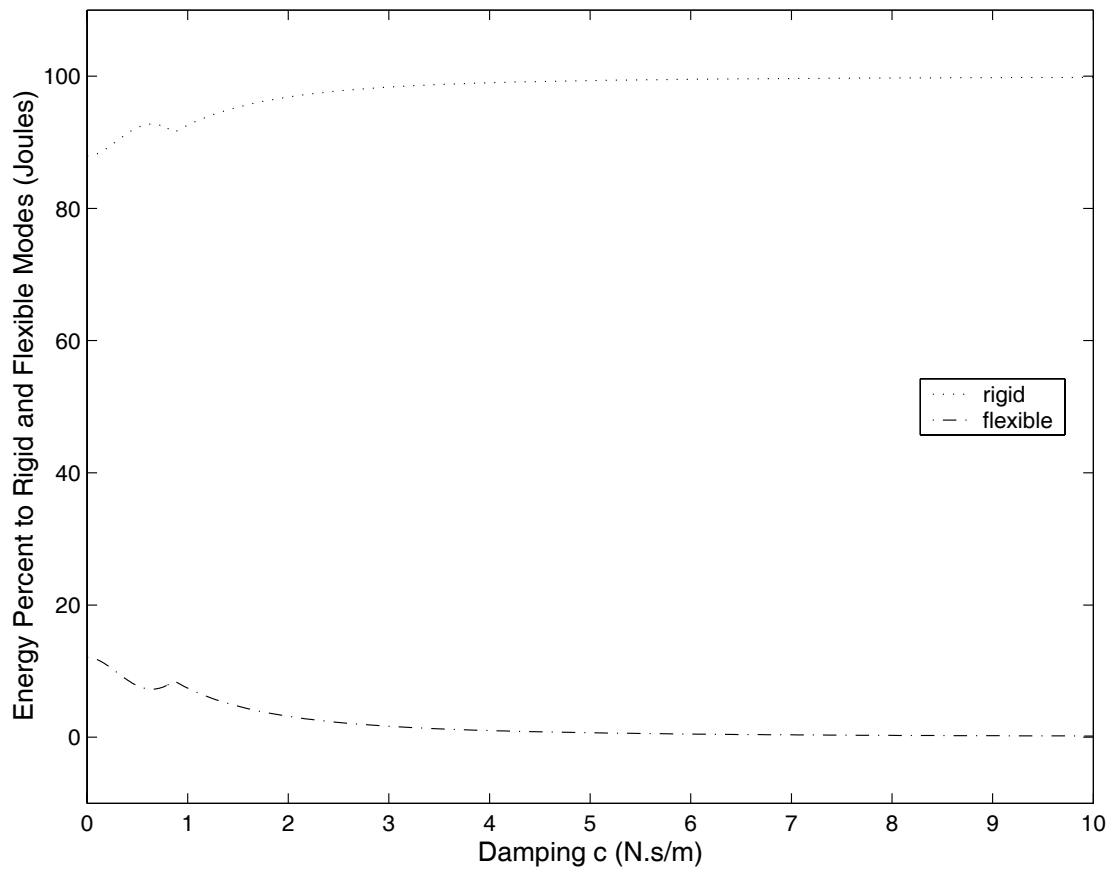


Fig. 10 Percentages of energy transfer to the rigid and flexible modes.

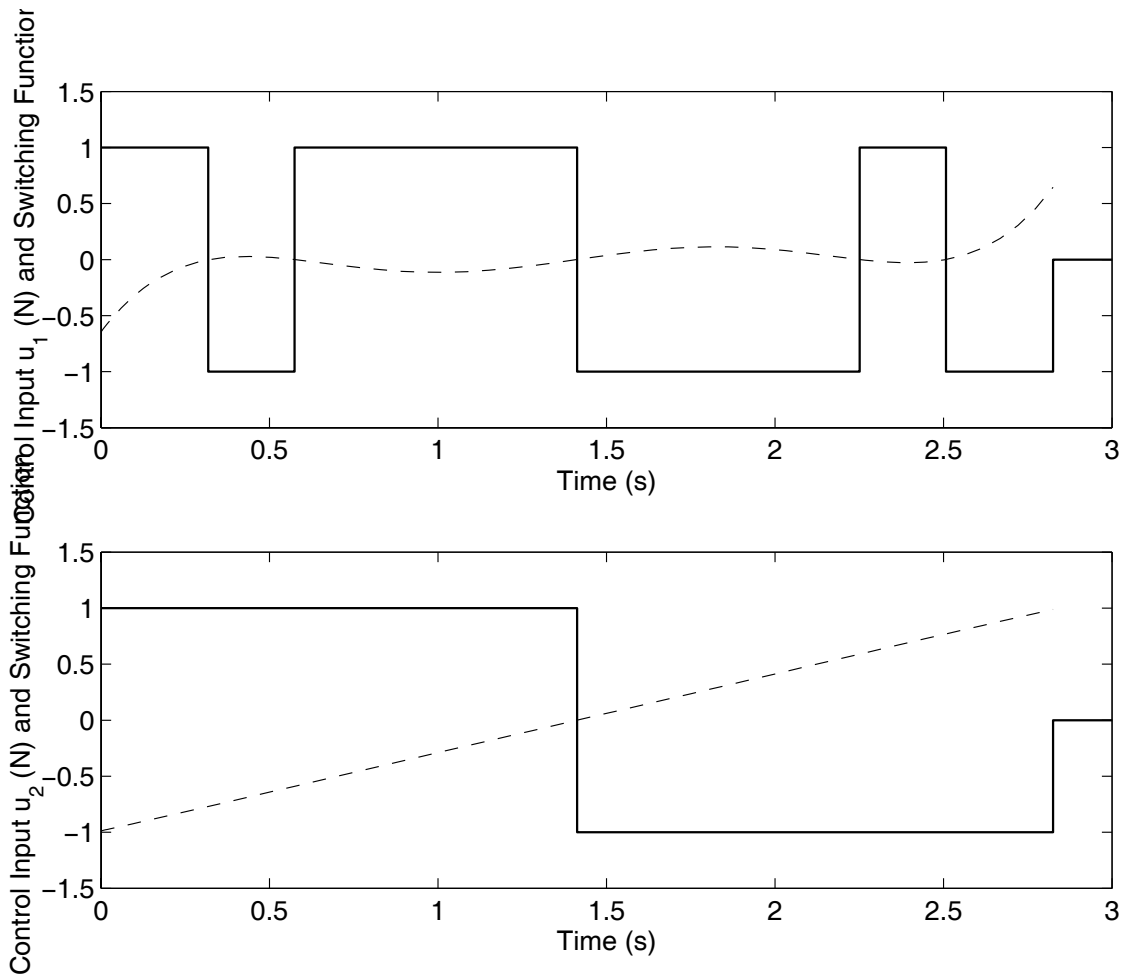


Fig. 11 Robust time-optimal control inputs and corresponding switching function.

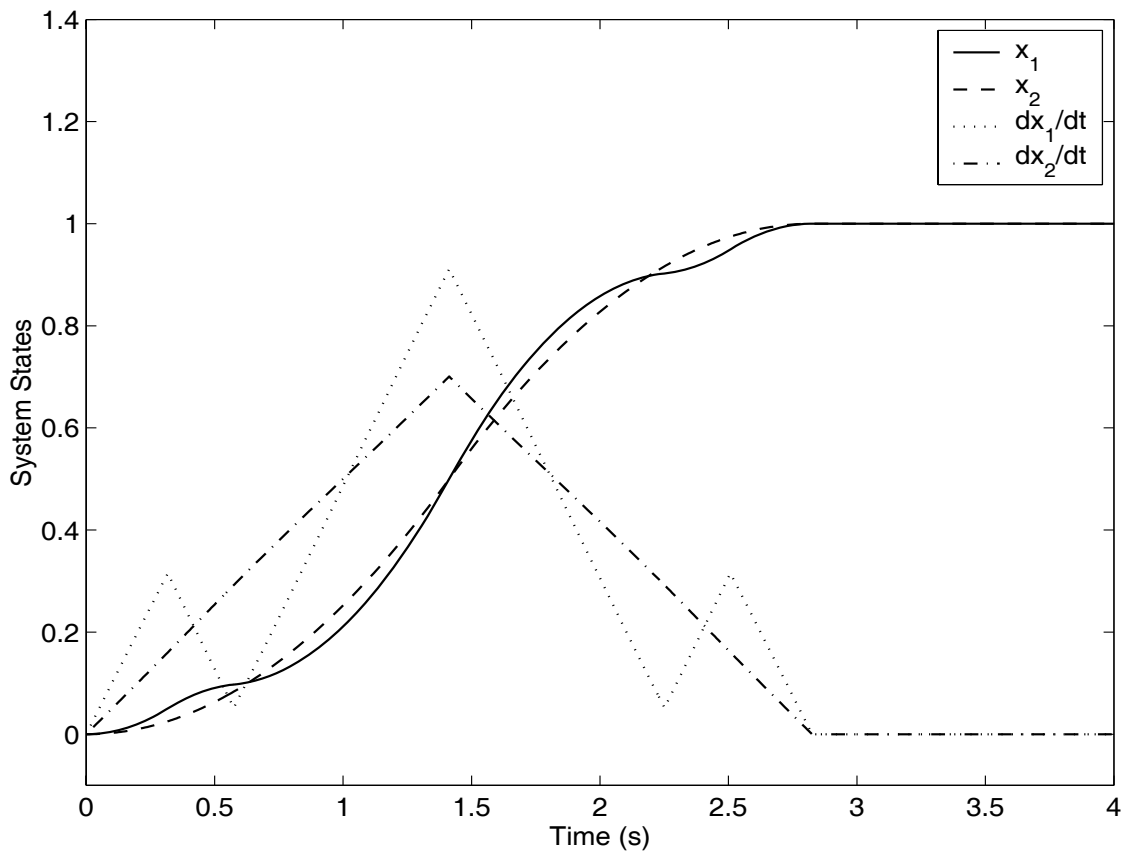


Fig. 12 Robust time-optimal state trajectories.

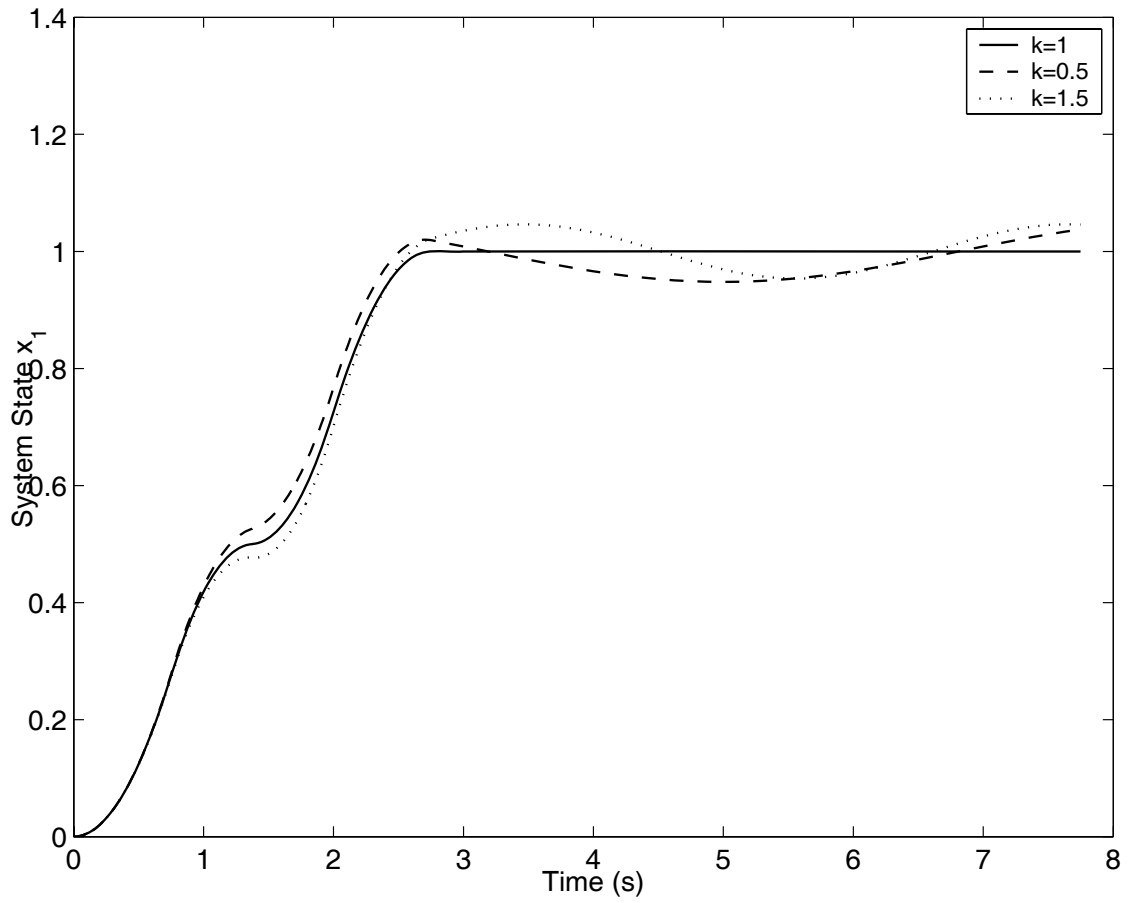


Fig. 13 State x_1 for different values of stiffness k – non robust case.

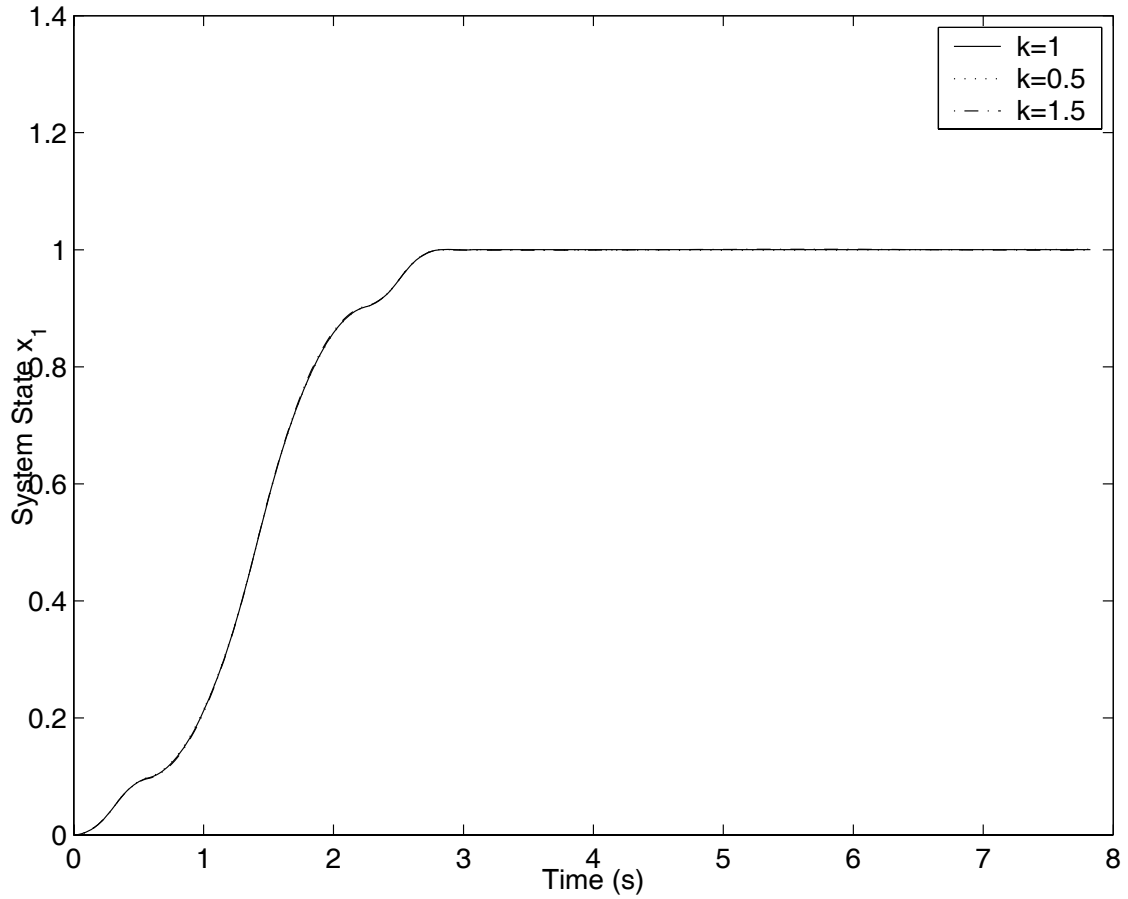


Fig. 14 State x_1 for different values of stiffness k – robust case.

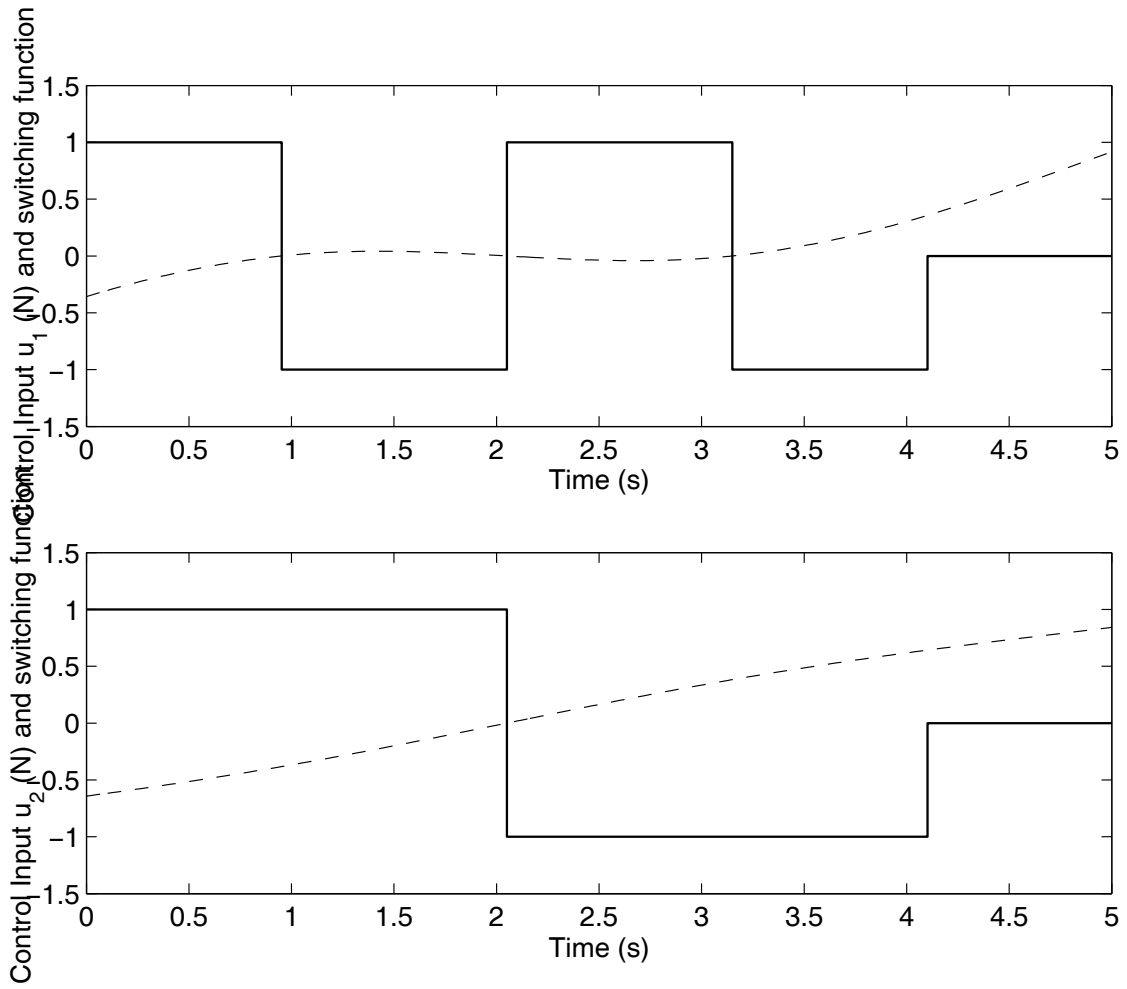


Fig. 15 Time Optimal Control Inputs u_1 and u_2 and corresponding switching functions.

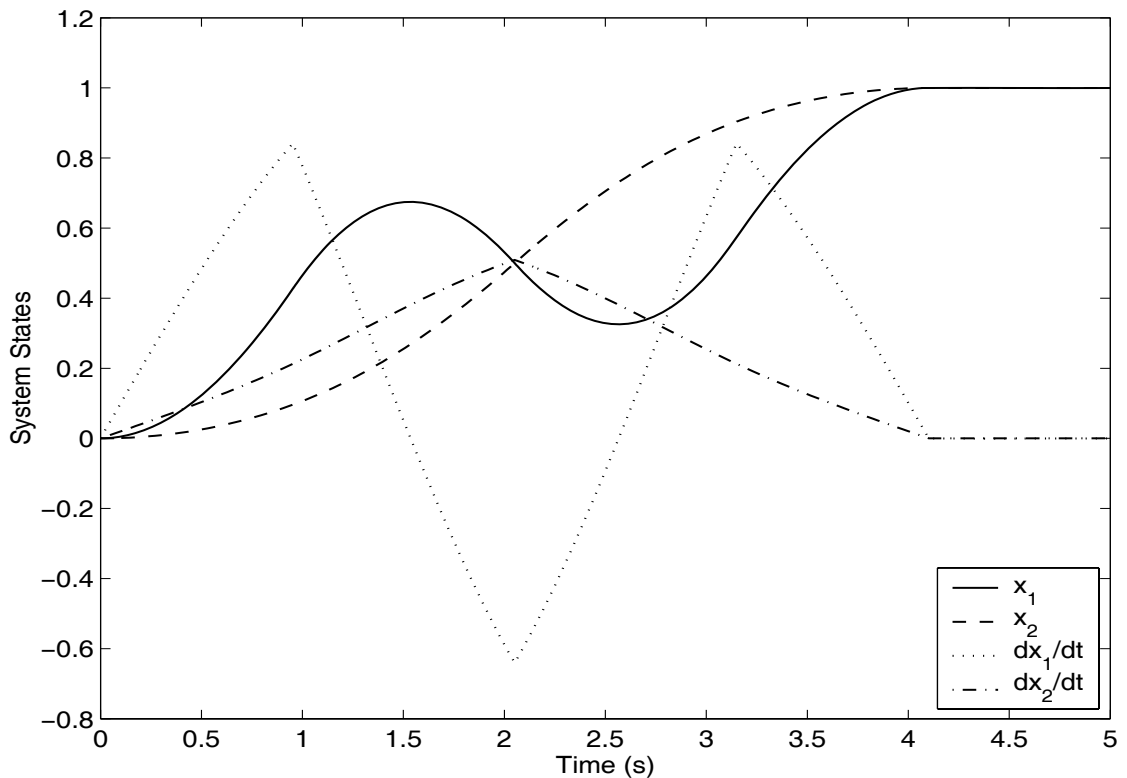


Fig. 16 Time-Optimal state trajectories for the nonlinear system.

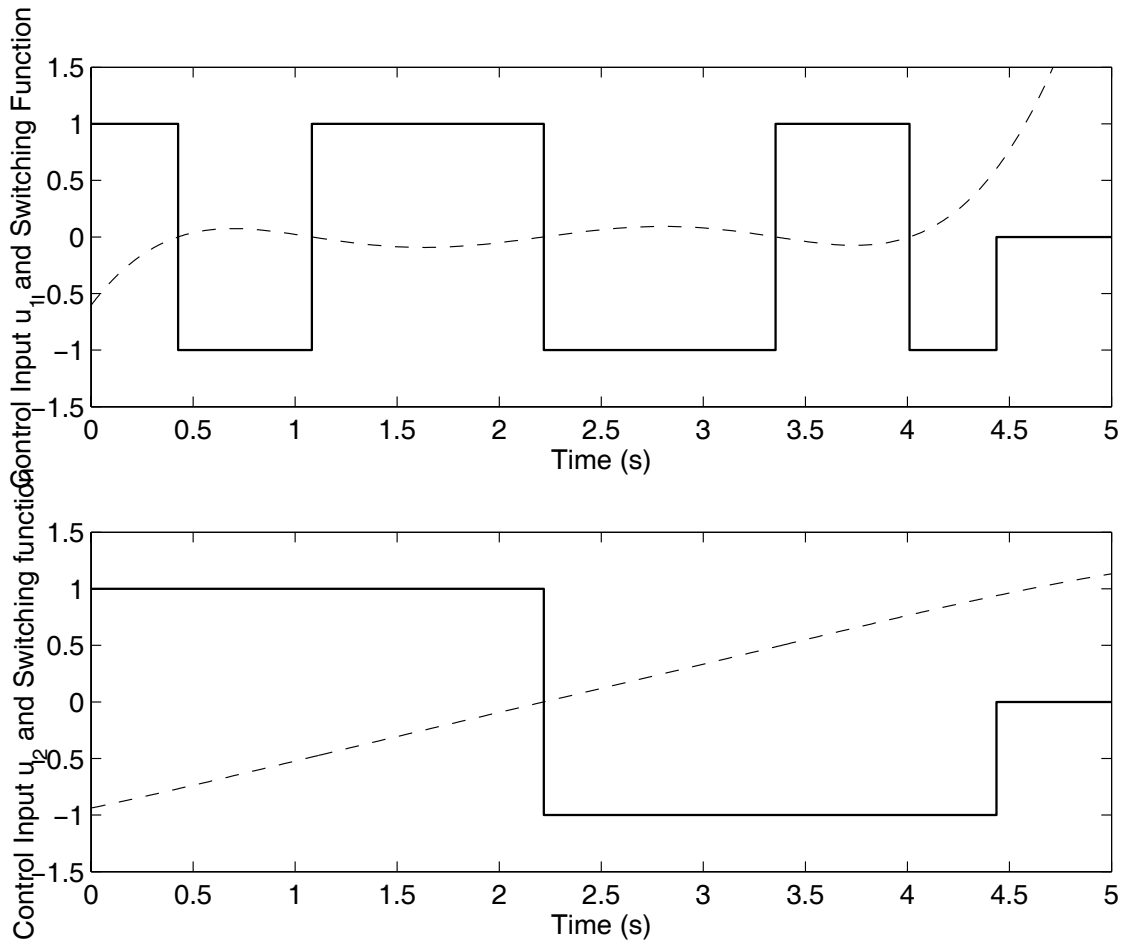


Fig. 17 Robust time-optimal control inputs u_1 and u_2 and corresponding switching functions.

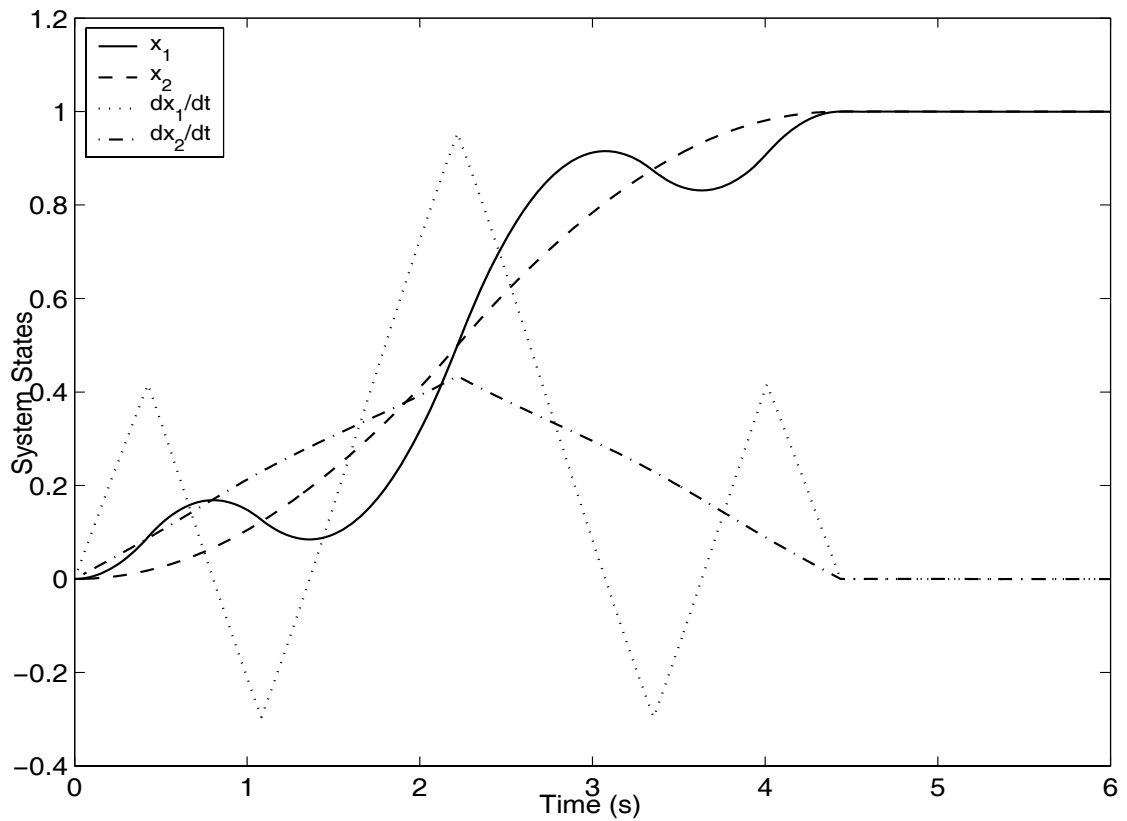


Fig. 18 Robust time-optimal state trajectories for the nonlinear system.

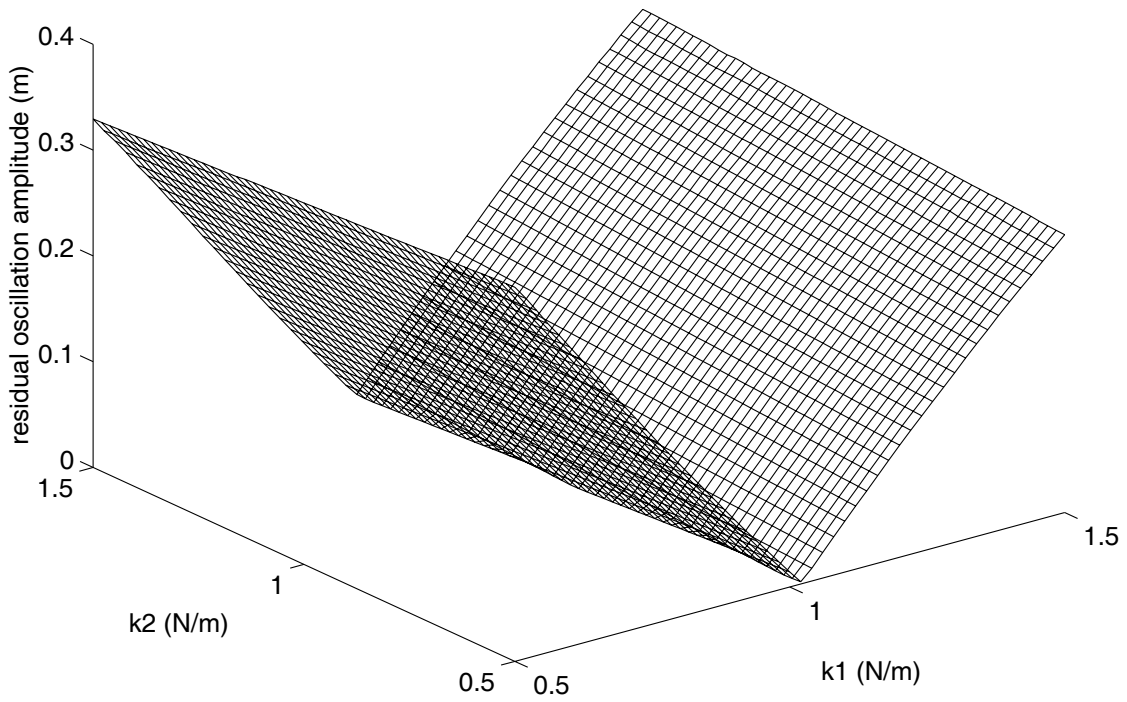


Fig. 19 Maximum residual oscillation amplitude of x_1 for the non-robust time-optimal design.

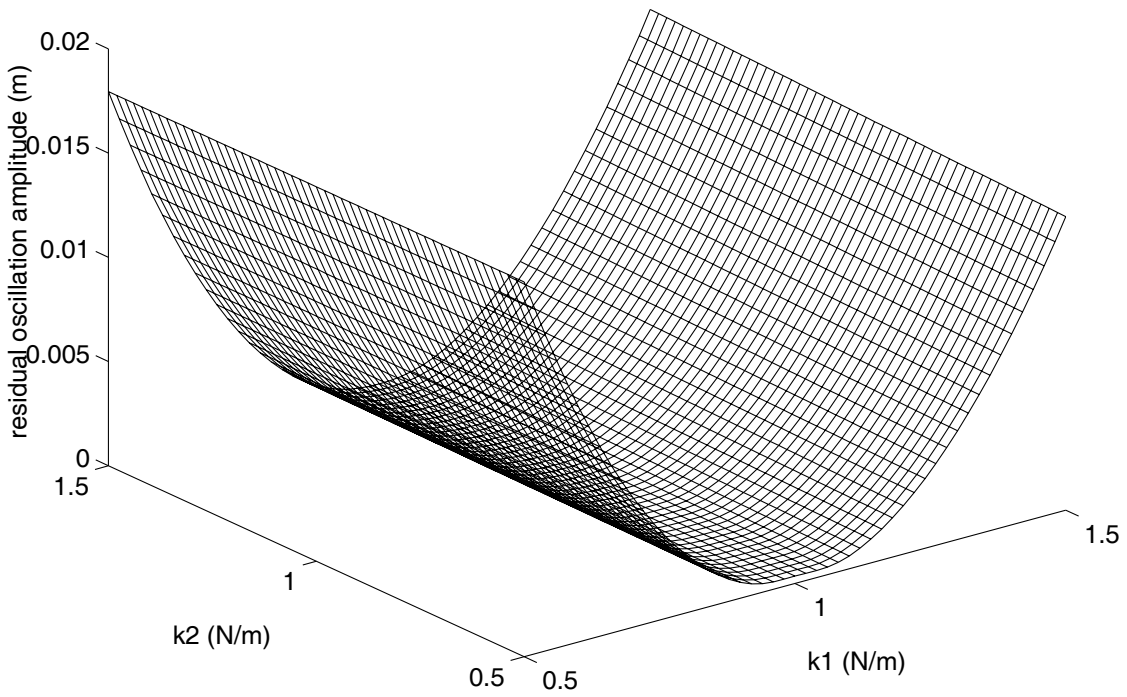


Fig. 20 Maximum residual oscillation amplitude of x_1 for the robust time-optimal design.